



## Whole-rock geochemistry of augen gneiss from southeast of Dumka, Jharkhand, India

Jimmy Lalnunmawia\*<sup>1</sup>, H. Thomas<sup>2</sup>, Shiva Kumar<sup>1</sup> and V. Vanthangliana<sup>1</sup>

<sup>1</sup>Department of Geology, Mizoram University, Aizawl 796 009, India

<sup>2</sup>Dr. Harisigh Gour Central University, Sagar (M.P.), India

Received 21 November 2010 | Revised 10 February 2011 | Accepted 14 February 2011

### ABSTRACT

The Chhotanagpur Granite Gneiss Complex (CGGC) exhibits various geological signatures that attract many geologist and researchers for detail investigation. The present paper focused on the petrography and geochemistry of augen gneiss exposed in the southeast of Dumka, Jharkhand. As in other areas of the CGGC, augen gneiss was the main rock exposure. They were coarse-grained and light colored rocks exhibiting well gneissic characteristics. The rock was mainly composed of quartz, feldspar, hornblende, pyroxene, biotite, garnet and other opaque minerals. It was also rich in alumina and potash contents. There was also a pronounced negative Eu anomaly which suggested that both K-feldspar and plagioclase were not removed in the differentiation sequence. As the whole CGGC experienced different orogenic activities, the studied rocks also showed various deformation effects. The augen gneiss was found to be originated from granite to granodioritic igneous parentage of calc-alkaline composition in the tectonic setting within plate granite.

**Key words:** Augen gneiss; CGGC; Dumka; petrography; rare earth elements; trace elements.

### INTRODUCTION

The Eastern Chhotanagpur Granite Gneiss Complex (CGGC) forms a very important segment of the Precambrian continental shield of eastern India. It has been inferred that the granite gneisses represent the basement, and that the schistose rocks of the supracrustals containing mafic enclaves were deformed and metamorphosed together, generally under am-

phibolite to locally granulite facies conditions.<sup>1</sup> The occurrences of basic granulites, charnockite and khondalite have been reported by different workers from the high-grade rocks of the area around Dumka.<sup>2,3</sup> The region may be taken as the type area of high-grade domains in the NE part of the CGGC.<sup>4</sup> The CGGC represent a number of linear E-W trending belts each with distinct petro-mineralogical and structural features. The present paper deals with the mineralogical compositions of the rock, source magma type and tectonic setting of the protolith.

Corresponding author: J. Lalnunmawia  
Phone: +91-09862329703  
E-mail: [c.lalbata2010@yahoo.in](mailto:c.lalbata2010@yahoo.in)

## MATERIALS AND METHODS

### Geological setting

The regional geological setting of the CGGC is shown in Figure 1.<sup>5,6</sup> The study area represents the eastern part of the CGGC which is characterized by a complex geological structures and different rock types of varying ages. The CGGC includes high grade metasediments, gneisses, migmatites, khondalite, leptynite, granulites and metagneous rocks, which have been intruded by mafic-ultramafic rocks, gabbro-anorthosite, granite, rapakivi granite, syenite, pegmatite, aplite and dolerite, tholeiitic basalts (Rajmahal Traps) at different geological periods.<sup>7-10</sup> The regional trend in the area varies from N-S in the west to E-W in the east-central part to ENE-WSW in the extreme east and numerous short and discontinuous shear zones are present almost throughout the area and have affected almost all the rock types which are indicated by the development of augens and mylonite banding.<sup>3</sup> This gneissic complex with an east-west regional strike was a composite terrain of deformed and predominantly amphibolite metamorphic sequence of silicic gneisses, migmatites interleaved with thin bands of supracrustals and acidic plutons.<sup>11</sup>

The CGGC is a vast tract of high-grade rocks and gneisses with enclaves of granulite

and metasedimentary rocks, and intrusive granites of Proterozoic age. The intrusions of mantle-derived rocks of varied composition ranging from mafic-ultramafic, sodic-ultrapotassic alkaline rocks, massif anorthosite to younger tholeiitic basalts (Rajmahal) and dolerite at different geological periods ranging from Late Palaeoproterozoic to Early Tertiary, give evidence of an active mantle in the prolonged history of evolution of this mobile belt.<sup>10</sup>

As in the rest of the CGGC, the most dominating rock type in the reported area was augen gneiss which is encountered around the southeastern side of Dumka town, Jharkhand. The rocks exhibited good gneissose structures and foliations were very well developed in which the dark band of the gneiss was composed of hornblende, pyroxene, biotite, garnet and Fe-oxide minerals, while the light bands were quartz and feldspar minerals. The augens in augen gneiss of the reported area were made up of either feldspar or aggregate of quartz and feldspar which were wrapped around by foliation in the rock. The augen structures were believed to be formed due to stretching of quartzofeldspathic layer during deformation.

### Sample analysis

The oxide percentage of major elements in

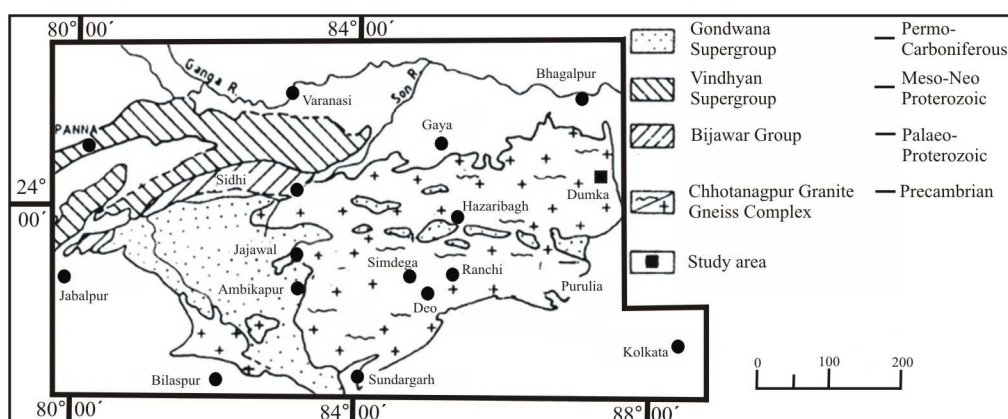


Figure 1. Regional geological map of the Chhotanagpur granite gneiss complex.

the rocks were analyzed by Philips MagiX PRO model PW 2440 wavelength dispersive X-ray fluorescence spectrometer coupled with automatic sample changer PW 2540 in National Geophysical Research Institute (NGRI), Hyderabad. The REE and trace elements were analyzed by Perkin Elmer SCIEX, Model ELAN® DRC II Inductively Coupled Plasma-Mass Spectrometer (ICP-MS) at NGRI, Hyderabad. The procedures followed in the preparation of the rock samples for analyses on XRF and ICP-MS were of national and international standards.<sup>12,13</sup>

## RESULTS AND DISCUSSIONS

### *Petrography*

The rock was composed mainly of feldspar, quartz, hypersthene, and hornblende with minor amounts of biotite. Besides the major mineral constituents stated above, the mineral phases that occur in the gneiss were garnet, ilmenite, magnetite, rutile and apatite. The ribbon structures of quartz due to deformation in the rock were very common (Figure 2a). Along the ribbon structure of quartz were

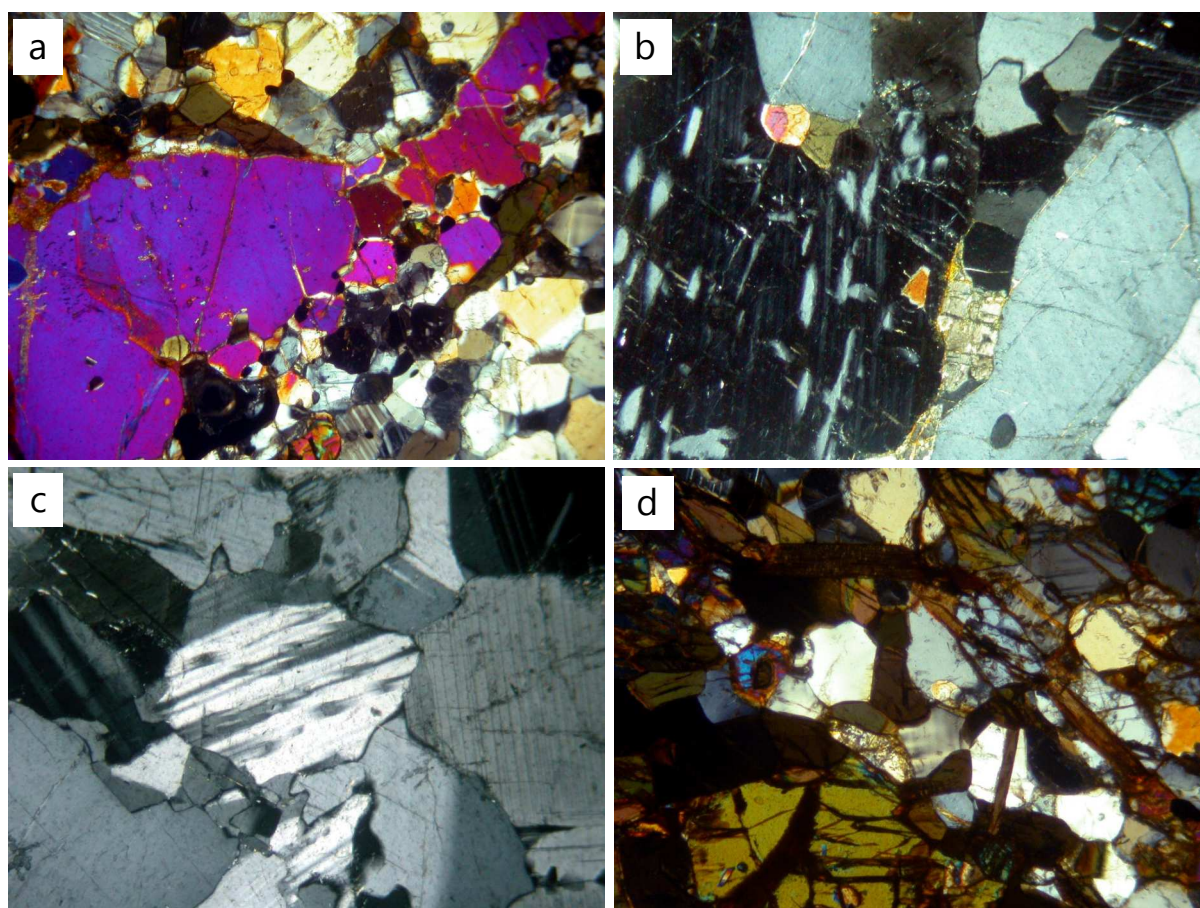


Figure 2. a) Ribbon structure in quartz was commonly observed in the rock; b) blebs of quartz in plagioclase indicate metasomatism; c) Deformed lamellae in plagioclase due to the effect of deformation in the rock ; d) Microcline was relatively negligible in the rock due to high temperature dominance during formation of the rock.

Table 1. Major element analyses (in wt%), and CIPW Norms values of augen gneiss from Dumka area, District Dumka, Jharkhand.

Ref. No.	1	2	3	4	5	6	7	8	9	10	11
Sample No.	D08	D14	D21	D23	D24	D25	D26	D27	D29	D52	D54
	Major Elements										
SiO <sub>2</sub>	66.47	64.76	61.53	64.55	66.51	62.67	59.92	64.73	62.91	61.57	63.19
Al <sub>2</sub> O <sub>3</sub>	14.55	14.26	14.66	14.54	15.12	15.22	13.75	14.17	14.02	14.9	16.69
FeO <sup>t</sup>	2.19	3.25	3.94	2.98	2.11	3.21	4.44	2.83	3.79	3.35	2.05
MnO	0.07	0.1	0.12	0.09	0.07	0.1	0.15	0.1	0.13	0.11	0.07
MgO	1.03	1.37	1.29	0.93	0.74	1.04	1.69	0.96	1.27	1.22	0.73
CaO	2.64	3.63	4.15	4.15	3.8	3.82	4.81	3.57	4.78	3.75	2.79
Na <sub>2</sub> O	2.07	2.59	2.7	2.87	2.75	2.6	2.75	2.55	3.13	2.64	2.51
K <sub>2</sub> O	6.15	3.7	3.19	3.84	4.04	4.32	3.01	4.63	1.93	4.84	7.09
TiO <sub>2</sub>	0.63	0.93	1.23	0.93	0.64	0.97	1.51	0.85	1.08	1.1	0.67
P <sub>2</sub> O <sub>5</sub>	0.26	0.33	0.54	0.42	0.32	0.47	0.67	0.42	0.43	0.47	0.32
Sum	98.737	98.901	98.153	98.976	98.668	98.355	98.117	98.267	98.097	98.054	98.598
	CIPW Norms										
Qz	24.02	26.04	23.66	24.1	26.33	22.04	21.49	24.08	26.19	18.86	14.96
Ab	17.52	21.92	22.85	24.29	23.27	22	23.27	21.58	26.49	22.34	21.24
An	11.4	15.85	17.06	15.45	16.76	15.88	16.28	13.54	18.5	14.51	11.75
Or	36.34	21.87	18.85	22.69	23.87	25.53	17.79	27.36	11.41	28.6	41.9
C	0.31	0.18	0.51	-	0.08	0.45	-	-	-	-	0.58
Di	-	-	-	1.93	-	-	2.57	1.15	1.94	0.82	-
Hy	3.46	4.74	4.67	2.45	2.67	3.82	4.44	2.96	3.81	3.8	2.54
Ilm	1.2	1.77	2.34	1.77	1.22	1.84	2.87	1.61	2.05	2.09	1.27
Mt	3.89	5.77	6.97	5.34	3.73	5.7	7.86	5.02	6.71	5.94	3.62
Ap	0.6	0.76	1.25	0.97	0.74	1.09	1.55	0.97	1	1.09	0.74
An %	39.42	41.96	42.75	38.88	41.87	41.92	41.16	30.01	41.12	39.37	35.62

Table 2. Trace elements and REE analyses (in ppm) of augen gneiss from Dumka area, District Dumka, Jharkhand.

Ref. No.	1	2	3	4	5	6	7	8	9	10	11
Sample No.	D08	D 14	D21	D23	D24	D25	D26	D27	D29	D52	D54
	Trace Elements										
Sc	5.91	7.76	7.10	6.62	4.92	7.19	7.94	6.84	7.50	7.08	5.05
V	34.97	54.02	50.87	40.58	29.63	43.68	59.03	36.15	51.34	43.37	31.79
Cr	4.29	5.14	5.08	5.04	4.11	5.18	5.44	4.55	5.20	4.96	4.14
Co	12.44	16.00	19.18	17.21	12.29	15.92	22.55	14.53	18.59	16.04	15.43
Ni	1.34	1.31	1.29	1.44	1.06	1.32	1.64	1.13	1.45	1.28	1.27
Cu	0.44	0.54	0.55	0.50	0.42	0.60	0.58	0.48	0.58	0.48	0.55
Zn	105.61	125.23	135.56	105.92	18.53	72.88	64.63	109.85	51.44	37.59	54.42
Ga	24.89	26.55	25.97	27.11	25.82	26.43	27.90	26.07	29.09	24.71	25.30
Rb	172.43	103.86	77.90	97.15	104.52	101.75	64.50	122.52	56.01	111.24	182.81
Sr	217.24	179.75	194.28	223.48	231.64	214.62	216.78	224.86	131.31	228.14	285.11
Y	37.86	40.60	45.15	39.22	30.86	42.50	57.84	39.13	61.96	44.58	30.75
Zr	55.95	53.22	88.80	65.38	52.56	61.54	84.79	60.77	74.60	61.80	53.15
Nb	16.69	20.02	27.78	24.65	18.09	25.21	32.14	24.28	25.96	26.08	18.82
Cs	1.60	0.78	0.48	0.53	0.64	0.56	0.45	0.80	0.54	0.41	0.61
Ba	2553.75	1436.48	1261.46	1549.48	1690.36	1706.80	1365.18	1893.27	546.59	1896.36	3087.17
Hf	1.75	1.68	2.74	2.16	1.70	2.17	2.33	2.13	2.20	1.98	1.74
Ta	0.54	0.51	0.67	0.65	0.52	0.72	0.39	0.96	0.70	0.89	0.79
Pb	15.76	11.98	11.73	11.26	10.41	11.72	10.40	15.35	10.01	11.28	15.78
Th	3.25	2.90	3.86	3.68	3.17	3.18	4.46	4.33	2.95	2.82	2.93
U	0.96	0.99	1.54	2.93	0.98	4.72	1.46	1.43	1.26	0.83	0.97

Table 2. Continued.

	Rare Earth Elements													
La	45.21	54.59	56.58	61.23	48.08	62.36	78.37	50.83	54.42	61.85	49.61			
Ce	82.55	105.97	115.11	123.39	88.60	121.09	162.58	113.74	118.58	126.55	114.82			
Pr	9.57	11.43	13.74	13.36	10.07	13.83	18.98	11.87	13.29	14.22	10.82			
Nd	40.21	48.02	60.14	57.04	42.33	59.30	81.01	50.61	58.29	60.41	44.51			
Sm	7.49	8.76	11.10	10.22	7.43	10.91	14.54	9.63	12.17	10.83	7.84			
Eu	2.97	2.36	2.65	2.89	2.74	2.90	2.92	2.87	2.20	2.80	3.29			
Gd	6.56	7.66	9.44	8.57	6.36	9.13	12.03	8.08	10.56	9.10	6.71			
Tb	1.03	1.15	1.37	1.21	0.92	1.30	1.74	1.22	1.73	1.31	0.95			
Dy	6.43	7.24	8.03	7.00	5.52	7.73	10.43	7.29	11.20	7.99	5.50			
Ho	0.74	0.79	0.87	0.75	0.60	0.83	1.11	0.75	1.21	0.85	0.59			
Er	2.50	2.66	2.91	2.55	2.03	2.74	3.67	2.56	4.00	2.87	2.00			
Tm	0.32	0.34	0.34	0.31	0.24	0.31	0.43	0.30	0.50	0.35	0.23			
Yb	3.14	3.28	3.55	2.91	2.34	3.03	4.26	2.89	4.92	3.32	2.29			
Lu	0.51	0.54	0.59	0.49	0.41	0.49	0.70	0.48	0.83	0.56	0.38			
ΣREE	209.22	254.77	286.42	291.92	217.64	295.95	392.77	263.11	293.90	302.98	249.53			
LREE/HRE	179.88	222.78	251.09	261.49	193.54	263.08	348.11	232.13	245.11	268.50	225.67			
(La/Yb) <sub>N</sub>	10.32	11.94	11.42	15.11	14.74	14.75	13.21	12.63	7.93	13.36	15.56			
La/Eu	15.24	23.09	21.33	21.19	17.55	21.49	26.82	17.74	24.71	22.10	15.08			
Eu/Lu	5.79	4.35	4.49	5.88	6.72	5.90	4.18	5.92	2.65	4.99	8.63			

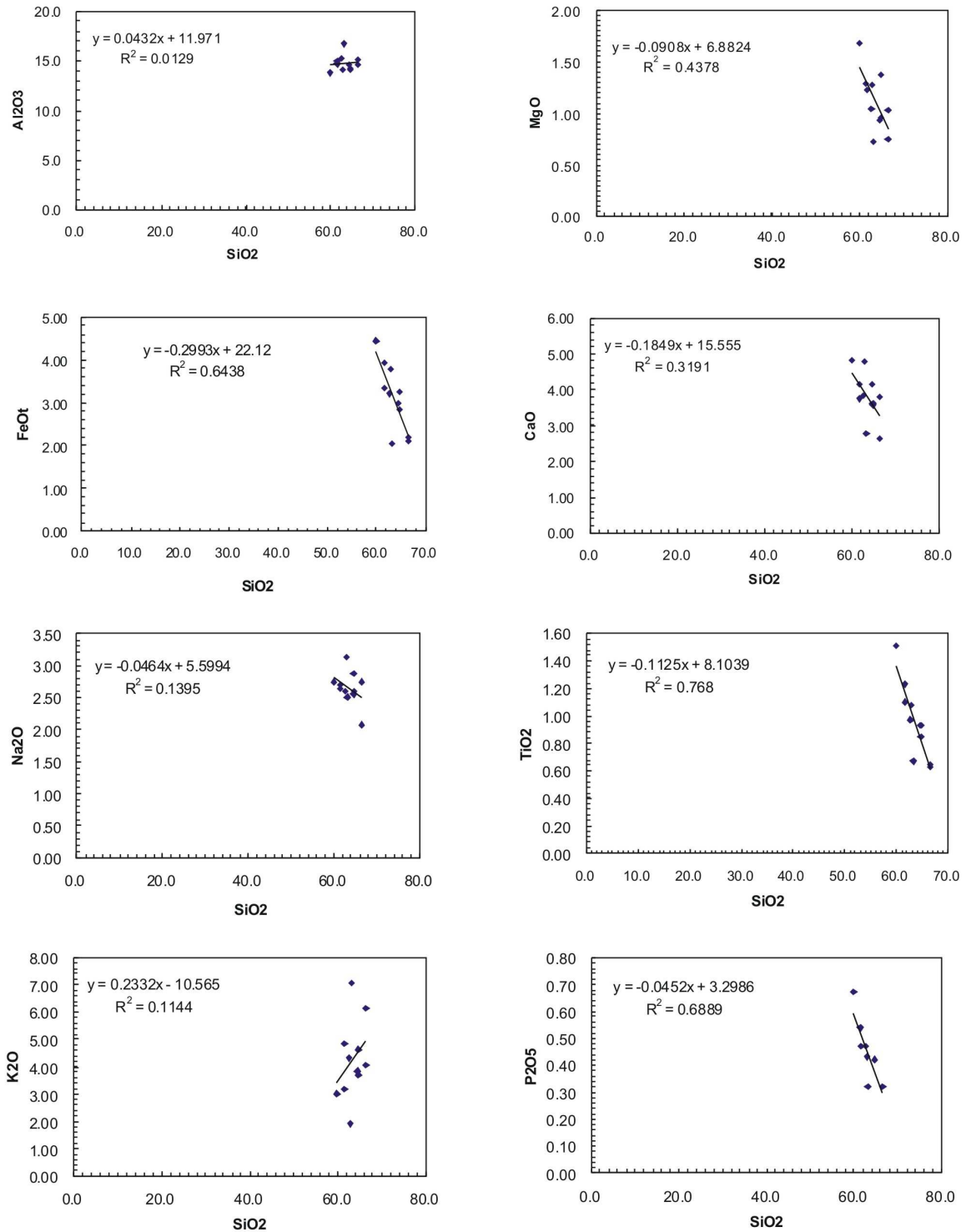


Figure 3. Harker's variation diagram.

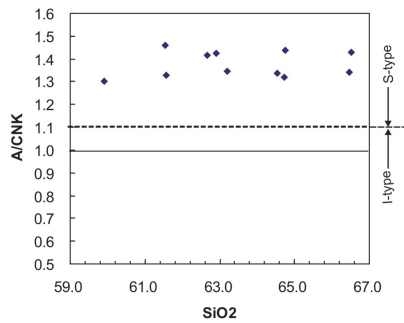


Figure 4. Chemical compositions of all the selected eleven samples of augen gneiss.

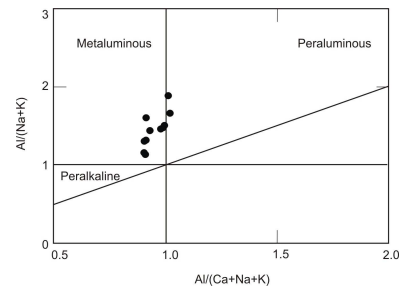


Figure 5. Al/(Ca+Na+K) versus Al/(Na+K) discrimination diagram of the selected eleven samples of augen gneiss.

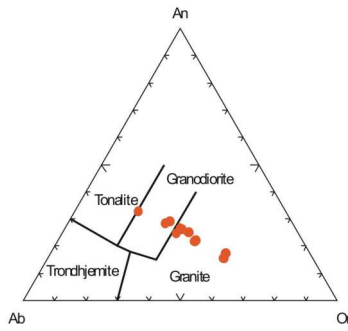


Figure 6. The system anorthite(An) – albite(Ab) – orthoclase (Or) showing the field of different granitic composition.

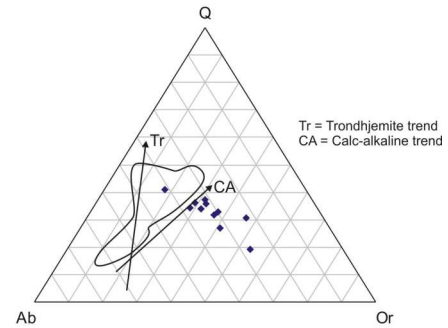


Figure 7. Qz-Ab-Or discriminative diagram of gneiss/augen gneiss.

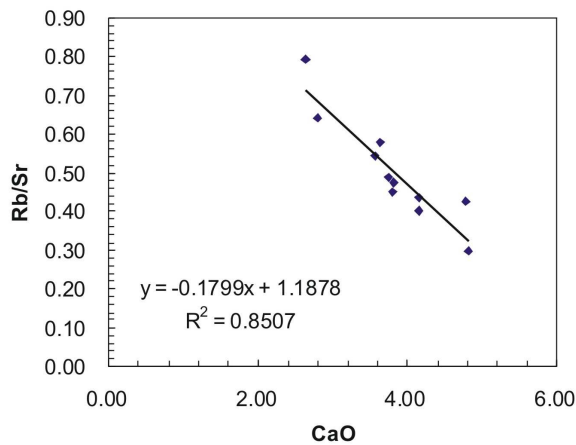


Figure 8. Rb/Sr versus CaO showing linear relationship of the selected eleven samples of augen gneiss.

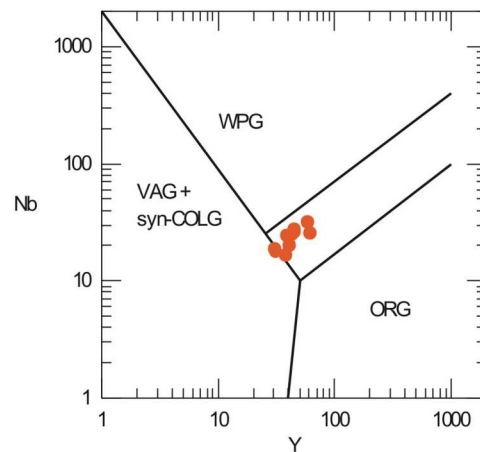


Figure 9. Y versus Nb discrimination diagram of the selected eleven samples of gneiss/augen



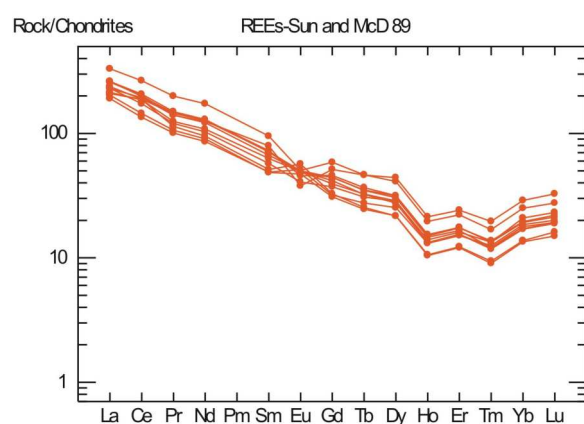


Figure 10. The Chondrite-normalized REE distribution diagram of the selected eleven samples of gneiss/augen gneiss.

aligned flakes of biotite, hornblende, orthopyroxene and garnet with ilmenite and magnetite. A compositional layering was conspicuous in thin sections of the rock.

Although the rock had undergone various deformation events, there were only a few reaction textures to be observed in the rock. The different mineral parageneses observed in the rock were:

1. Plagioclase-orthopyroxene-K-feldspar-biotite-hornblende-garnet-perthite-quartz-ilmenite.
2. Plagioclase-K-feldspar-orthopyroxene-hornblende-garnet-perthite-quartz-magnetite-ilmenite.

Orthopyroxene occurred as short prismatic form having two sets of cleavages with typical schiller's structures. Quartz usually occurred as tiny small inclusion in plagioclase which suggests the influence of metasomatism or hydrothermal action (Figure 2b). They were also exhibiting undulose extinction which indicates post crystalline deformation. Post crystallization phenomena in the rock were also indicated by deformed lamellae in plagioclase (Figure 2c). Microclines were relatively

negligible compared to other feldspar group of minerals which indicate high temperature regime in the evolution of augen gneiss in the area of investigation (Figure 2d). Biotites show strong preferred orientation, occasionally in two directions. Ilmenite and magnetite were the most commonly observed opaque minerals in the rock.

#### *Petrochemistry and petrogenesis*

The results of chemical analyses on major oxides, trace elements and REE for the eleven selected augen gneiss assemblages are shown in Tables 1 and 2. The rocks of different assemblages showed clear chemical differences. The compositional range for major elements was displayed in Harker variation diagrams (Figure 3). The  $\text{SiO}_2$  contents of gneiss range from 59.92 to 66.51 % averaging at 63.53%. With increasing  $\text{SiO}_2$  content,  $\text{Al}_2\text{O}_3$ ,  $\text{FeO}$ , and  $\text{MgO}$  markedly decreased from 16.69 to 13.75%, 3.94 to 2.05% and 1.37 to 0.73%, respectively. The  $\text{K}_2\text{O}$  varied from 1.93 to 7.09 % and averaged at 4.25%; while  $\text{Na}_2\text{O}$  ranged from 2.07 to 3.13% with an average of 2.65%. The  $\text{CaO}$  content ranged from 2.64 to 4.78% averaging at 3.81%. The  $\text{K}_2\text{O}$ ,  $\text{Na}_2\text{O}$  and  $\text{CaO}$  contents were positively correlated with  $\text{SiO}_2$ . The melting of (hydrated) basaltic rocks yielded granodiorite to tonalite magma with low  $\text{MgO}$  (commonly <2%) and  $\text{SiO}_2$  >~60%.<sup>14,15</sup> All the gneissic samples fall in the same range and an origin by partial melting of oceanic crust during subduction.<sup>16</sup>

The gneiss of the study area had S-type of character (molecular  $\text{Al}_2\text{O}_3/(\text{K}_2\text{O}+\text{Na}_2\text{O}+\text{CaO}) >1.1$ ) with normative corundum and normative diopside (Figure 4).<sup>17</sup> The plot between  $\text{Al}/(\text{Ca}+\text{Na}+\text{K})$  versus  $\text{Al}/(\text{Na}+\text{K})$  clearly indicated that the samples fall within the field of meta- to peraluminous (Figure 5).<sup>18</sup> The An-Ab-Or diagram shown in Figure 6 clearly indicated that all the samples lie within the granite and granite to granodiorite field.<sup>19</sup> The Qz-Ab-Or discriminative diagram also clearly indicated that all samples lie

within the field of calc-alkaline (Figure 7).<sup>20</sup>

The plot between Rb/Sr versus CaO was shown in Figure 8 showed linear trend which was indicating progressive partial melting and fractional crystallization.<sup>31</sup> The Y versus Nb diagram basically constructed for the discrimination of different field of origin of granites was shown in Figure 9.<sup>22</sup> The plots revealed that the gneissic assemblage falls within the fields of within plate granite.

The study of REE analyses provides valuable information about the source. During metamorphism the REE were highly fractionated and also immobile during sedimentary processes.<sup>23-25</sup> During metamorphism the REE remain unaffected up to the upper amphibolite facies regional metamorphism.<sup>26</sup> On the other hand REEs have been shown to be a bit mobile during metamorphism.<sup>24,27,28</sup> The rare earth data for gneissic assemblages were normalized to chondrites.<sup>29</sup> Their values are plotted in Figure 10. It was observed from this figure that LREE pattern (with La/Eu ratio 20.58) were steeper than the HREEs (with Eu/Lu ratio of 4.51). However, a pronounced negative europium (Eu) anomaly was present in all the samples with an average concentration of 2.78 ppm. The negative Eu anomaly suggested that the parent magma was being depleted in Eu with favor of feldspar differentiation, and that may also be indicative of requiring silica-rich parent liquid. The slightly enriched heavy rare earth element (HREE) pattern may be explained due to the higher abundance of garnet in the gneiss.<sup>30</sup> For the gneissic assemblages, it has been observed that the total value of REE ranges from 209.22 to 392.77 ppm. The ratio of LREE/HREE varies from 179.88 to 348.11 ppm and the (La/Yb)<sub>N</sub> ratio varies from 7.93 to 15.56. The pattern of REE, along with the LREE/HREE and (La/Yb)<sub>N</sub> ratio suggests towards strong fractionation. The very high Ba, Sr and LREE have been found suggesting participation of a strongly enriched mantle source in the petrogenesis of this rocks.<sup>31</sup>

## CONCLUSION

On the basis of above discussion, it is clear that the augen gneiss of the study area had S-type of character (molecular  $Al_2O_3/(K_2O+Na_2O+CaO) > 1.1$ ) and their parent rock may be granite to granodioritic in nature whose composition was akin to calc-alkaline. The graphical representations and interpretation of the chemical analyses clearly showed that the rock was originated in the tectonic setting of Within Plate Granite environment. They may be the product of progressive partial melting and fractional crystallization of oceanic crust during subduction. This conclusion was also supported by the petrographic observation such as the presence of blebs of quartz in plagioclase which was due to metasomatism or hydrothermal influences. The high concentration of trace elements such as Ba and Sr, and the LREE suggested the participation of a highly enriched mantle source in the petrogenesis of this gneissic rock.

## ACKNOWLEDGEMENT

The authors are grateful to the Council of Scientific and Industrial Research (CSIR), New Delhi for the financial support. The authors also thank Department of Geology, Mizoram University for providing facilities to carry out the research.

## REFERENCES

1. Bhattacharya DS, Ghosal A & Ravi Kant V (1990). Chhotanagpur Granite Gneiss in relation to the schistose rocks around Murhu, Ranchi district, Bihar: a structural approach. *Proc Indian Acad Sci*, **99**, 269-277.
2. Bhattacharya BP (1976). Metamorphism of Precambrian rocks of the central part of Santhal Parganas District, Bihar. *Bull Geol Min Soc Ind*, **48**, 183-196.
3. Barman TR, Bishui PK, Mukhopadhyay K & Ray JN (1994). Rb-Sr geochronology of the high-grade rocks from Prulia, West Bengal and Jamua-Dumka Sector, Bihar. *Indian Miner*, **48**, 45-60.
4. Mahadevan TM (2002). *Geology of Bihar and Jharkhand*.

- Geological Society of India Bangalore, India, pp. 563.
5. Ghose NC (1983). Geology, tectonics and evolution of the Chhotanagpur granite gneiss complex, eastern India. In: *Recent Researches in Geology 10*. Hindustan Publications Corporation, New Delhi, pp. 211-247.
  6. Rai SD, Shivananda SR, Tiwary KN, Banerjee DC & Kaul R (1991). Xenotime-bearing inland placers in India and their beneficiation. *Explor Res At Miner*, **4**, 77-92.
  7. Mukherjee D & Ghose NC (1992). Precambrian anorthosites within the Chhotanagpur Gneissic Complex. *Indian J Geol*, **64**, 143-150.
  8. Mukherjee D & Ghose NC (1999). Damodar graben: A centre of contrasting magmatism in the eastern Indian shield margin. In: *Basement Tectonics 13* (AK Sinha, ed). Kluwer Academic Publishers, Netherlands, pp. 179-202.
  9. Ghose NC & Mukherjee D (2000). Chhotanagpur gneiss-granulites complex, Eastern India-A kaleidoscope of global events. In: *Geology and Mineral Resources of Bihar and Jharkhand, Platinum Jubilee Commemorative Volume* (AN Trivedi, BC Sarkar, NC Ghose & YR Dhar, eds). Indian School of Mines, Dhanbad, Institutional Geoexploration and Environment Monograph 2, Patna, pp. 33-58.
  10. Ghose NC, Mukherjee D & Chatterjee N (2005). Plume generated Mesoproterozoic mafic-ultramafic magmatism in the Chhotanagpur mobile belt of eastern Indian Shield Margin. *J Geol Soc Ind*, **66**, 725-740.
  11. Naha K & Mukhopadhyay D (1990). Structural styles in the Precambrian metamorphic terranes of peninsular India: A synthesis. In: *Precambrian Continental Crust and Its Mineral Resources* (SM Naqvi, ed). Elsevier, Amsterdam, pp. 156-178.
  12. Chao TT & Sanzalone RF (1992). Decomposition techniques. *J Geochem Explor*, **44**, 65-106.
  13. Roy P, Balaram V & Kumar A (2007). New REE and trace element data on two kimberlitic reference materials by ICP-MS. *Geostand Geoanal Res*, **31**, 261-273.
  14. Rapp RP, Watson EB & Miller CF (1991). Partial melting of amphibolite/eclogite and the origin of Archaean trondhjemite and tonalite. *Precambrian Res*, **51**, 1-25.
  15. Wyllie PJ, Wolf MB & van der Laan SR (1997). Conditions for formation of tonalities and trondhjemites: magmatic sources and products. In: *Greenstone Belts* (M De Wit & LD Ashwall, eds). *Oxford Monographs on Geology and Geophysics*, **35**, 256-266.
  16. Barkar F & Arth JG (1976). Generation of trondhjemitic tonalitic liquids and Archaean bimodal trondhjemite basalt suites. *Geology*, **4**, 596-600.
  17. Chappel BW & White AJR (1974). Two contrasting granite types. *Pacific Geol*, **8**, 173-174.
  18. Maniar PD & Piccoli PM (1989). Tectonic discrimination of granitoids. *Bull Geol Soc Amer*, **101**, 635-643.
  19. Barkar F (1979). Trondhjemite: Definition, environment and hypotheses of origin. In: *Trondhjemite, Dacites and Related Rocks* (F Barkar, ed). Elsevier, Amsterdam, pp. 1-22.
  20. Larsen ES (1948). Batholith and associated rocks of Corom, Elsinore, and San Luis Rey quadrangles, southern California. *Geol Soc Amer Mem*, **29**, 182.
  21. Robb LJ (1983). Trace element trends in granites and the distinction between partial melting and crystal fractionation processes. Case studies from two granites in southern Africa. In: *The significance of Trace Elements in Solving Petrogenetic Problems and Controversies* (SS Augustithis, ed). Theophrastus Publications, Athens, pp. 279-294.
  22. Pearce JA, Harris NBW & Tindle AG (1984). Trace element discrimination diagrams for the tectonic interpretation of granitic rocks. *J Petrol*, **25**, 956-983.
  23. Chaudhuri S & Cullers RL (1979). The distributions of rare earth elements in deeply buried Gulf Coast sediments. *Chem Geol*, **24**, 327-338.
  24. McLennan SM (1982). On the geochemical evolution of sedimentary rocks. *Chem Geol*, **37**, 335-350.
  25. Fleet AJ (1984). Aqueous and sedimentary geochemistry of rare earth elements. In: *Rare Earth Element Geochemistry* (P Henderson, ed). Elsevier, Amsterdam, pp. 343-373.
  26. Taylor SR & McLennan SM (1985). *The Continental Crust: Its Composition and Evolution*. Blackwell, London, pp. 312.
  27. Muecke GK, Pride C & Sarkar P (1979). Rare earth element geochemistry of regional metamorphic rocks. *Phys Chem Earth*, **11**, 449-464.
  28. Humphries SE (1984). The mobility of rare earth elements in the crust. In: *Rare Earth Element Geochemistry* (P Henderson, ed). Elsevier, Amsterdam, pp. 317-342.
  29. Sun SS & McDonough WF (1989). Chemical and isotopic systematics of oceanic basalts: implications for mantle composition and processes. In: *Magmatism in Ocean Basins* (AD Saunders, & MJ Norry, eds). Geological Society of London Special Publication, 42, pp. 313-345.
  30. Rao PV, Nageswara, Rao AT & Yoshida M (1996). Geochemical characters of leptynites from the Visakhapatnam area in the Eastern Ghats granulite terrane, India. *J South-east Asian Earth Sci*, **14**, 199-207.
  31. Steenfelt A (1997). High Ba-Sr-LREE-P components in Early Proterozoic magmas within the Nagssugtoqidian orogen, West Greenland. *Terra Nova*, **9**, 360.